

Measurement of Time-Dependent CP -Violating Parameters in $B^0 \rightarrow K_S^0 K_S^0$ Decays

Y. Nakahama,⁴¹ K. Sumisawa,⁷ I. Adachi,⁷ H. Aihara,⁴¹ T. Aushev,^{17,12} A. M. Bakich,³⁸ V. Balagura,¹² E. Barberio,²⁰ I. Bedny,¹ K. Belous,¹¹ U. Bitenc,¹³ A. Bondar,¹ A. Bozek,²⁶ M. Bračko,^{19,13} T. E. Browder,⁶ P. Chang,²⁵ Y. Chao,²⁵ A. Chen,²³ K.-F. Chen,²⁵ W. T. Chen,²³ B. G. Cheon,⁵ R. Chistov,¹² I.-S. Cho,⁴⁶ Y. Choi,³⁷ J. Dalseno,²⁰ M. Dash,⁴⁵ A. Drutskoy,³ S. Eidelman,¹ N. Gabyshev,¹ B. Golob,^{18,13} H. Ha,¹⁵ J. Haba,⁷ K. Hara,²¹ T. Hara,³¹ K. Hayasaka,²¹ M. Hazumi,⁷ D. Heffernan,³¹ Y. Hoshi,⁴⁰ Y. B. Hsiung,²⁵ H. J. Hyun,¹⁶ T. Iijima,²¹ K. Inami,²¹ A. Ishikawa,³⁴ H. Ishino,⁴² R. Itoh,⁷ M. Iwasaki,⁴¹ Y. Iwasaki,⁷ D. H. Kah,¹⁶ H. Kaji,²¹ J. H. Kang,⁴⁶ N. Katayama,⁷ H. Kawai,² T. Kawasaki,²⁸ H. Kichimi,⁷ H. J. Kim,¹⁶ H. O. Kim,¹⁶ Y. J. Kim,⁴ K. Kinoshita,³ S. Korpar,^{19,13} P. Križan,^{18,13} P. Krokovny,⁷ R. Kumar,³² C. C. Kuo,²³ A. Kuzmin,¹ Y.-J. Kwon,⁴⁶ J. Lee,³⁶ J. S. Lee,³⁷ M. J. Lee,³⁶ S. E. Lee,³⁶ T. Lesiak,²⁶ A. Limosani,²⁰ S.-W. Lin,²⁵ D. Liventsev,¹² F. Mandl,¹⁰ S. McOnie,³⁸ T. Medvedeva,¹² W. Mitaroff,¹⁰ K. Miyabayashi,²² H. Miyata,²⁸ Y. Miyazaki,²¹ R. Mizuk,¹² G. R. Moloney,²⁰ E. Nakano,³⁰ M. Nakao,⁷ H. Nakazawa,²³ Z. Natkaniec,²⁶ S. Nishida,⁷ O. Nitoh,⁴⁴ T. Nozaki,⁷ S. Ogawa,³⁹ T. Ohshima,²¹ S. Okuno,¹⁴ S. L. Olsen,^{6,9} H. Ozaki,⁷ P. Pakhlov,¹² G. Pakhlova,¹² C. W. Park,³⁷ H. Park,¹⁶ K. S. Park,³⁷ R. Pestotnik,¹³ L. E. Piilonen,⁴⁵ H. Sahoo,⁶ Y. Sakai,⁷ O. Schneider,¹⁷ C. Schwanda,¹⁰ A. J. Schwartz,³ R. Seidl,^{8,33} M. E. Seviar,²⁰ M. Shapkin,¹¹ C. P. Shen,⁹ H. Shibuya,³⁹ J.-G. Shiu,²⁵ B. Shwartz,¹ J. B. Singh,³² A. Somov,³ S. Stanič,²⁹ M. Starič,¹³ T. Sumiyoshi,⁴³ O. Tajima,⁷ F. Takasaki,⁷ N. Tamura,²⁸ M. Tanaka,⁷ G. N. Taylor,²⁰ Y. Teramoto,³⁰ I. Tikhomirov,¹² K. Trabelsi,⁷ T. Tsuboyama,⁷ S. Uehara,⁷ K. Ueno,²⁵ T. Uglov,¹² Y. Unno,⁵ S. Uno,⁷ Y. Ushiroda,⁷ G. Varner,⁶ K. Vervink,¹⁷ C. H. Wang,²⁴ P. Wang,⁹ X. L. Wang,⁹ Y. Watanabe,¹⁴ E. Won,¹⁵ Y. Yamashita,²⁷ Y. Yusa,⁴⁵ Z. P. Zhang,³⁵ A. Zupanc,¹³ and O. Zyukova¹

(The Belle Collaboration)

¹*Budker Institute of Nuclear Physics, Novosibirsk*

²*Chiba University, Chiba*

³*University of Cincinnati, Cincinnati, Ohio 45221*

⁴*The Graduate University for Advanced Studies, Hayama*

⁵*Hanyang University, Seoul*

⁶*University of Hawaii, Honolulu, Hawaii 96822*

⁷*High Energy Accelerator Research Organization (KEK), Tsukuba*

⁸*University of Illinois at Urbana-Champaign, Urbana, Illinois 61801*

⁹*Institute of High Energy Physics, Chinese Academy of Sciences, Beijing*

¹⁰*Institute of High Energy Physics, Vienna*

¹¹*Institute of High Energy Physics, Protvino*

¹²*Institute for Theoretical and Experimental Physics, Moscow*

¹³*J. Stefan Institute, Ljubljana*

¹⁴*Kanagawa University, Yokohama*

¹⁵*Korea University, Seoul*

¹⁶*Kyungpook National University, Taegu*

¹⁷*École Polytechnique Fédérale de Lausanne (EPFL), Lausanne*

¹⁸*Faculty of Mathematics and Physics, University of Ljubljana, Ljubljana*

¹⁹*University of Maribor, Maribor*

²⁰*University of Melbourne, School of Physics, Victoria 3010*

²¹*Nagoya University, Nagoya*

²²*Nara Women's University, Nara*

²³*National Central University, Chung-li*

²⁴*National United University, Miao Li*

²⁵*Department of Physics, National Taiwan University, Taipei*

²⁶*H. Niewodniczanski Institute of Nuclear Physics, Krakow*

²⁷*Nippon Dental University, Niigata*

²⁸*Niigata University, Niigata*

²⁹*University of Nova Gorica, Nova Gorica*

³⁰*Osaka City University, Osaka*

³¹*Osaka University, Osaka*

³²*Panjab University, Chandigarh*

³³*RIKEN BNL Research Center, Upton, New York 11973*

³⁴*Saga University, Saga*

³⁵University of Science and Technology of China, Hefei³⁶Seoul National University, Seoul³⁷Sungkyunkwan University, Suwon³⁸University of Sydney, Sydney, New South Wales³⁹Toho University, Funabashi⁴⁰Tohoku Gakuin University, Tagajo⁴¹Department of Physics, University of Tokyo, Tokyo⁴²Tokyo Institute of Technology, Tokyo⁴³Tokyo Metropolitan University, Tokyo⁴⁴Tokyo University of Agriculture and Technology, Tokyo⁴⁵Virginia Polytechnic Institute and State University, Blacksburg, Virginia 24061⁴⁶Yonsei University, Seoul

(Received 27 December 2007; published 27 March 2008)

We report a measurement of the CP -violating parameters in $B^0 \rightarrow K_S^0 K_S^0$ decays based on a data sample of $657 \times 10^6 B\bar{B}$ pairs collected at the $Y(4S)$ resonance with the Belle detector at the KEKB asymmetric-energy e^+e^- collider. In this Letter, one neutral B meson is fully reconstructed in the $B^0 \rightarrow K_S^0 K_S^0$ decay mode, and the flavor of the accompanying B meson is identified by its decay products. The CP -violating parameters are measured from the asymmetry in the distributions of the proper-time interval between the two B decays: $\mathcal{S}_{K_S^0 K_S^0} = -0.38_{-0.77}^{+0.69}(\text{stat}) \pm 0.09(\text{syst})$ and $\mathcal{A}_{K_S^0 K_S^0} = -0.38 \pm 0.38(\text{stat}) \pm 0.05(\text{syst})$.

DOI: 10.1103/PhysRevLett.100.121601

PACS numbers: 11.30.Er, 12.15.Hh, 13.25.Hw

B^0 meson decays proceeding via flavor-changing $b \rightarrow d\bar{q}q$ or $s\bar{q}q$ transitions are sensitive to new physics (NP) contributions affecting the internal quark loop diagrams. Such NP contributions can add new weak phases and subsequently cause deviations from the standard model (SM) expectations for CP -violating parameters [1].

The decay $B^0 \rightarrow K_S^0 K_S^0$ is dominated by $b \rightarrow d\bar{s}s$ transitions. The SM predicts that the CP -violating parameters $\mathcal{S}_{K_S^0 K_S^0}$ and $\mathcal{A}_{K_S^0 K_S^0}$ are zero in the limit that the top quark dominates and the contribution from internal up and charm quark exchanges in the loop diagram is small [2]. On the other hand, NP can enhance the $\mathcal{S}_{K_S^0 K_S^0}$ and $\mathcal{A}_{K_S^0 K_S^0}$ values [3], so their measurements are sensitive probes of NP. The parameter $\mathcal{S}_{K_S^0 K_S^0}$ arises from interference between a mixing-induced amplitude and a nonmixed decay amplitude while the parameter $\mathcal{A}_{K_S^0 K_S^0}$ arises from CP violation in the decay amplitude itself. Experimentally, there are no prompt charged tracks from the B vertex for a $B^0 \rightarrow K_S^0 K_S^0$ decay, and hence the B decay vertex must be reconstructed by using K_S^0 's that decay inside the vertex detector and a constraint on the beam interaction point (IP). Both CP -violating parameters have previously been measured by the *BABAR* collaboration; they obtained a large $\mathcal{S}_{K_S^0 K_S^0}$ value, albeit with a large statistical error [4]. In this Letter, we report a measurement of $\mathcal{S}_{K_S^0 K_S^0}$ and $\mathcal{A}_{K_S^0 K_S^0}$ in $B^0 \rightarrow K_S^0 K_S^0$ decays using almost twice the statistics of the previous measurement. Our analysis is based on $657 \times 10^6 B\bar{B}$ pairs collected with the Belle detector [5] running at the KEKB asymmetric-energy e^+e^- (3.5 on 8 GeV) collider [6].

In the decay chain $Y(4S) \rightarrow B\bar{B} \rightarrow (K_S^0 K_S^0) f_{\text{tag}}$, where one of the B mesons decays at time $t_{K_S^0 K_S^0}$ to $K_S^0 K_S^0$ and the other decays at time t_{tag} to a flavor specific state f_{tag} that

distinguishes between B^0 and \bar{B}^0 , the decay rate has a time dependence [7] given by

$$\mathcal{P}_{K_S^0 K_S^0}(\Delta t) = \frac{e^{-|\Delta t|/\tau_{B^0}}}{4\tau_{B^0}} [1 + q\{\mathcal{S}_{K_S^0 K_S^0} \sin(\Delta m_d \Delta t) + \mathcal{A}_{K_S^0 K_S^0} \cos(\Delta m_d \Delta t)\}], \quad (1)$$

where $\Delta t = t_{K_S^0 K_S^0} - t_{\text{tag}}$, τ_{B^0} is the B^0 lifetime, Δm_d is the mass difference between the two B mass eigenstates, and $q = +1$ (-1) for $f_{\text{tag}} = B^0$ (\bar{B}^0).

At the KEKB, the $Y(4S)$ resonance is produced with a Lorentz boost of $\beta\gamma = 0.425$ nearly along the $+z$ axis, which is defined as the direction antiparallel to the e^+ beamline. Since the B^0 and \bar{B}^0 mesons are approximately at rest in the $Y(4S)$ center-of-mass system (CMS), Δt can be determined from the displacement in z between the $K_S^0 K_S^0$ and f_{tag} decay vertices: $\Delta t \simeq (z_{K_S^0 K_S^0} - z_{\text{tag}})/(\beta\gamma c) \equiv \Delta z/(\beta\gamma c)$.

The Belle detector is a large-solid-angle magnetic spectrometer that consists of a silicon vertex detector (SVD), a 50-layer central drift chamber, an array of aerogel threshold Cherenkov counters, a barrel-like arrangement of time-of-flight scintillation counters, and an electromagnetic calorimeter, which are located inside a superconducting solenoid coil that provides a 1.5 T magnetic field. An iron flux return located outside of the coil is instrumented to detect K_L^0 mesons and to identify muons. Two inner detector configurations were used. A 2.0 cm-radius beam pipe and a 3-layer SVD (SVD1) was used for the first data sample of $152 \times 10^6 B\bar{B}$ pairs, while a 1.5 cm-radius beam pipe, a 4-layer SVD (SVD2) [8], and a small-cell inner drift chamber were used to record the remaining $505 \times 10^6 B\bar{B}$ pairs.

We reconstruct a $K_S^0 \rightarrow \pi^+ \pi^-$ candidate from a pair of oppositely charged tracks having $|\Delta M_{K_S^0}| < 0.015 \text{ GeV}/c^2$ corresponding to 3 standard deviations (σ), where $\Delta M_{K_S^0}$ is the difference between their invariant mass and the nominal K_S^0 mass [9]. The impact parameters of both charged tracks are required to be more than $100 \mu\text{m}$. The angle in the transverse plane between the K_S^0 momentum vector and the direction defined by the K_S^0 vertex and the IP should be less than 50 mrad . In order to suppress incorrect combinations of the two charged tracks, the mismatch in the z direction at the K_S^0 vertex point for the two charged tracks is required to be less than 15 cm .

To identify $B^0 \rightarrow K_S^0 K_S^0$ decay candidates, we use two kinematic variables: the energy difference $\Delta E \equiv E_B^{\text{CMS}} - E_{\text{beam}}^{\text{CMS}}$ and the beam-energy constrained mass $M_{\text{bc}} \equiv \sqrt{(E_{\text{beam}}^{\text{CMS}})^2 - (p_B^{\text{CMS}})^2}$, where $E_{\text{beam}}^{\text{CMS}}$ is the beam energy in the CMS and E_B^{CMS} and p_B^{CMS} are the CMS energy and momentum, respectively, of reconstructed B candidates. We select candidates satisfying $|\Delta E| < 0.20 \text{ GeV}$ and $5.20 \text{ GeV}/c^2 < M_{\text{bc}} < 5.30 \text{ GeV}/c^2$. For the Δt fit described below, we use candidates in a signal region defined as $|\Delta E| < 0.10 \text{ GeV}$ and $5.27 \text{ GeV}/c^2 < M_{\text{bc}} < 5.30 \text{ GeV}/c^2$. We find that 0.2% of the selected events have multiple $B^0 \rightarrow K_S^0 K_S^0$ candidates. In such events, we choose the $B^0 \rightarrow K_S^0 K_S^0$ candidate having the smallest $\Sigma(\Delta M_{K_S^0})^2$ value.

To suppress continuum $e^+ e^- \rightarrow q\bar{q}$ ($q = u, d, s, c$) events, we form a likelihood \mathcal{L}_{sig} (\mathcal{L}_{bkg}) for signal (continuum) events by combining a Fisher discriminant based on modified Fox-Wolfram moments [10] with the probability density function (PDF) for the cosine of the CMS B^0 flight direction with respect to the $+z$ axis. The former makes use of the difference in event shapes: signal events have a spherical topology while background events tend to be jetlike. We impose a requirement on the likelihood ratio $\mathcal{R} = \mathcal{L}_{\text{sig}}/(\mathcal{L}_{\text{sig}} + \mathcal{L}_{\text{bkg}}) > 0.25$ that retains 89% of the signal and rejects 71% of the continuum.

The b flavor of the accompanying B meson is identified from inclusive properties of particles that are not associ-

ated with the reconstructed $B^0 \rightarrow K_S^0 K_S^0$ candidate. The tagging information is represented by two parameters: q , as defined in Eq. (1), and r , which is an event-by-event Monte Carlo-determined flavor-tagging dilution factor that ranges from $r = 0$ for no flavor discrimination to $r = 1$ for unambiguous flavor assignment [11]. Candidate events are selected to have $r > 0.1$, and are further divided into six r intervals. The wrong tag fraction w for each r interval and the differences Δw between B^0 and \bar{B}^0 decays are determined using semileptonic and hadronic $b \rightarrow c$ decay data [11].

The dominant background is continuum. We find the $B\bar{B}$ decay background contribution to be negligibly small using a large sample of GEANT-based Monte Carlo (MC) simulated events [12]. Thus, we take into account only signal and continuum events in the nominal fit. The uncertainty due to a possible contribution from $B\bar{B}$ decay background is included in the systematic errors.

The signal yield is extracted using a three-dimensional extended unbinned maximum likelihood (UML) fit to ΔE - M_{bc} - \mathcal{R} distributions for the selected candidate events. For the signal component, we model the ΔE (M_{bc}) shape using a sum of two Gaussians (a single Gaussian). A binned histogram is employed for the \mathcal{R} distribution. The parameters of the Gaussians and \mathcal{R} distribution are obtained using MC simulation. For the background component, the ΔE (M_{bc}) shape is modeled as a first-order polynomial (an ARGUS [13]) function. The parameters of these functions are floated in the fit. The \mathcal{R} background distribution is obtained from a data sample in the sideband region ($M_{\text{bc}} < 5.26 \text{ GeV}/c^2$). We form the likelihood from the product of ΔE , M_{bc} , and \mathcal{R} PDFs. Possible correlations among ΔE , M_{bc} , and \mathcal{R} are found to be negligible for signal events from the signal MC, and to be very small for continuum events from the data sideband. We include the effect of the small correlations in the latter in the systematic errors. The fit yields 58 ± 11 signal events among 476 $B^0 \rightarrow K_S^0 K_S^0$ candidate events in the signal region, where the error is statistical only. Figure 1 shows the projections of the ΔE , M_{bc} , and \mathcal{R} distributions for the candidate events. The signal component shown in Figs. 1(a) and

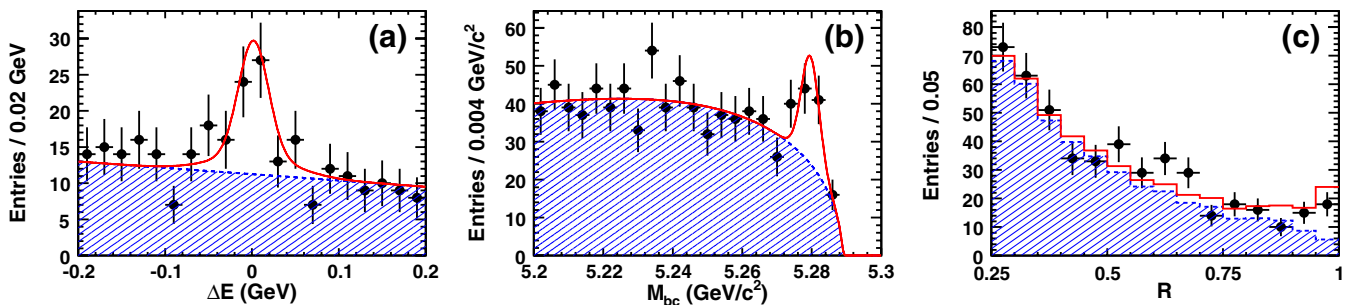


FIG. 1 (color online). (a) ΔE , (b) M_{bc} , and (c) \mathcal{R} projections for the $B^0 \rightarrow K_S^0 K_S^0$ candidate events (a) with $\mathcal{R} > 0.6$ and $5.27 \text{ GeV}/c^2 < M_{\text{bc}}$, (b) with $\mathcal{R} > 0.6$ and $|\Delta E| < 0.1 \text{ GeV}$, and (c) in the signal region. The solid histogram and curves show the fit projections and the hatched areas show the background component. The points with error bars are the data.

1(b) is 77% of the total signal due to the additional \mathcal{R} requirement.

We apply the B decay vertex reconstruction algorithm of Ref. [14]. The vertex position for a $B^0 \rightarrow K_S^0 K_S^0$ decay is obtained using the $K_S^0 \rightarrow \pi^+ \pi^-$ momentum vector and a constraint on the transverse components of the IP; the IP profile ($\sigma_x \approx 100 \mu\text{m}$, $\sigma_y \approx 5 \mu\text{m}$) is smeared by the finite B^0 flight length in the plane perpendicular to the z axis. To reconstruct the $B^0 \rightarrow K_S^0 K_S^0$ decay position, both charged pions from at least one of the K_S^0 's are required to have a sufficient number of hits in the SVD: at least one layer with hits on both the z and r - ϕ sides and at least one additional layer with a hit on the z side among the other layers for SVD1, and at least two layers with hits on both sides for SVD2. Both K_S^0 's are used for the vertex reconstruction if the four pions have a sufficient number of hits in the SVD. The typical vertex reconstruction efficiency with SVD1 (SVD2) is determined to be 44% (61%) from the signal MC. The vertex position resolutions in the z direction with SVD1 (SVD2) are $73 \mu\text{m}$ ($105 \mu\text{m}$) for the case where both K_S^0 's are used for the vertex reconstruction, and $141 \mu\text{m}$ ($172 \mu\text{m}$) for the case where a single K_S^0 is used. The latter resolution is comparable to the f_{tag} vertex position resolution. The B decay vertex in the tagside is determined from well-reconstructed tracks that are not assigned to the $B^0 \rightarrow K_S^0 K_S^0$ decay. The typical vertex reconstruction efficiency for f_{tag} decays is determined to be 93%.

We determine $\mathcal{S}_{K_S^0 K_S^0}$ and $\mathcal{A}_{K_S^0 K_S^0}$ by performing an UML fit to the Δt distribution. For signal events, we use the Δt distribution of Eq. (1), modified to include the effect of incorrect flavor assignment. The distribution $\mathcal{P}_{K_S^0 K_S^0}(\Delta t)$ is then convolved with the resolution function $R_{\text{sig}}(\Delta t)$, which depends on the event-by-event vertex position errors [15]; the dependence is calibrated using a $B^0 \rightarrow J/\psi K_S^0$ data control sample, where the vertex positions are reconstructed using only a K_S^0 and the IP profile [14]. We determine the following likelihood value for each event i :

$$P_i = (1 - f_{\text{ol}}) \int [f_{K_S^0 K_S^0} \mathcal{P}_{K_S^0 K_S^0}(\Delta t') R_{\text{sig}}(\Delta t_i - \Delta t') + (1 - f_{K_S^0 K_S^0}) \mathcal{P}_{q\bar{q}}(\Delta t') R_{q\bar{q}}(\Delta t_i - \Delta t')] d(\Delta t') + f_{\text{ol}} \mathcal{P}_{\text{ol}}(\Delta t_i), \quad (2)$$

where the PDF $\mathcal{P}_{\text{ol}}(\Delta t)$ is a broad Gaussian that represents an outlier component with a small fraction f_{ol} [15]. The fraction $f_{K_S^0 K_S^0}$ is the event-by-event signal fraction depending on ΔE , M_{bc} , and \mathcal{R} . We also take into account the r dependence of the signal fraction $f_{K_S^0 K_S^0}$; we determine the dependence using the signal MC and the sideband events for the signal and background components, respectively. For background events, the Δt distribution $\mathcal{P}_{q\bar{q}}(\Delta t)$ is convolved with a function $R_{q\bar{q}}(\Delta t)$, where the distribution $\mathcal{P}_{q\bar{q}}(\Delta t)$ is modeled as a sum of an exponential function and a delta function, and the function $R_{q\bar{q}}(\Delta t)$ is the sum of two Gaussians. All parameters in $\mathcal{P}_{q\bar{q}}(\Delta t)$ and $R_{q\bar{q}}(\Delta t)$ are determined from sideband events. We fix τ_{B^0} and Δm_d to their world-average values [9]. To improve the statistical sensitivity to $\mathcal{A}_{K_S^0 K_S^0}$, we also use candidate events having no Δt information, where both K_S^0 's decay outside the SVD and we do not reconstruct B vertices; for these events, we use the PDF of Eq. (2) integrated over Δt . The only free parameters in the fit are $\mathcal{S}_{K_S^0 K_S^0}$ and $\mathcal{A}_{K_S^0 K_S^0}$, which are determined by maximizing the likelihood function $L = \prod P_i$, where the product is over all events. The fit to 476 $B^0 \rightarrow K_S^0 K_S^0$ candidate events, in which 216 candidate events have no Δt information, yields

$$\mathcal{S}_{K_S^0 K_S^0} = -0.38^{+0.69}_{-0.77}(\text{stat}) \pm 0.09(\text{syst}), \quad (3)$$

and

$$\mathcal{A}_{K_S^0 K_S^0} = -0.38 \pm 0.38(\text{stat}) \pm 0.05(\text{syst}), \quad (4)$$

where the systematic errors are described below. Figure 2 shows the Δt distribution and raw asymmetry \mathcal{A}_{CP} in each Δt interval, where $\mathcal{A}_{CP} = (N_+ - N_-)/(N_+ + N_-)$

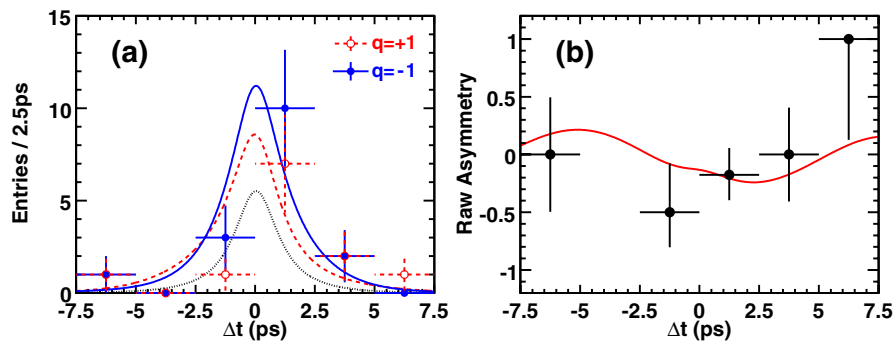


FIG. 2 (color online). (a) Δt distribution and (b) raw asymmetry \mathcal{A}_{CP} for the $B^0 \rightarrow K_S^0 K_S^0$ candidate events in the signal region with good tags ($r > 0.5$) and $\mathcal{R} > 0.6$. In (a), the dashed and solid curves show the fit results with $q = \pm 1$, respectively. The dotted curve shows the background component. In (b), the solid curve shows the fit projection.

and $N_{+(-)}$ is the number of candidate events with $q = +1$ (-1). Note that the signal component shown in Figs. 2(a) and 2(b) is 46% of the total signal with Δt information due to the additional requirements on r and \mathcal{R} .

The systematic error is primarily due to uncertainties in the parameters of $R_{\text{sig}}(\Delta t)$ (± 0.06 on $\mathcal{S}_{K_S^0 K_S^0}$ and < 0.01 on $\mathcal{A}_{K_S^0 K_S^0}$) and uncertainties in the signal fraction $f_{K_S^0 K_S^0}$ (± 0.04 on $\mathcal{S}_{K_S^0 K_S^0}$ and ± 0.03 on $\mathcal{A}_{K_S^0 K_S^0}$). We estimate a systematic error (± 0.04 on $\mathcal{S}_{K_S^0 K_S^0}$ and ± 0.02 on $\mathcal{A}_{K_S^0 K_S^0}$) for uncertainties in the parameters of $\mathcal{P}_{q\bar{q}}(\Delta t)$ and $R_{q\bar{q}}(\Delta t)$ and the possible contribution of, and asymmetry in, the $B\bar{B}$ decay background. The other contributions to the systematic errors come from uncertainties in the wrong tag fraction (± 0.02 on $\mathcal{S}_{K_S^0 K_S^0}$, ± 0.01 on $\mathcal{A}_{K_S^0 K_S^0}$), fit biases (± 0.02 , ± 0.01), physics parameters (τ_{B^0} and Δm_d) (± 0.01 , ± 0.01), the vertex reconstruction (± 0.01 , ± 0.02), and the tagside interference effect [16] (< 0.01 , ± 0.03). Adding all these contributions in quadrature, we obtain systematic errors of ± 0.09 for $\mathcal{S}_{K_S^0 K_S^0}$ and ± 0.05 for $\mathcal{A}_{K_S^0 K_S^0}$.

Various validity checks for the measurement are performed. We measure a branching fraction for $B^0 \rightarrow K^0 \bar{K}^0$ of $[1.1 \pm 0.2(\text{stat})] \times 10^{-6}$, which is consistent with our previous measurement [17]. The B^0 lifetime for the $B^0 \rightarrow K_S^0 K_S^0$ candidate events is measured to be 1.58 ± 0.44 ps, consistent with the world-average value [9]. We also fit to the sideband events of the $B^0 \rightarrow K_S^0 K_S^0$ data sample and find no CP asymmetry. Using MC pseudoexperiments, we find that the statistical errors obtained in our measurement are consistent with expectations. We apply the same procedure to the $B^0 \rightarrow J/\psi K_S^0$ data sample without using the J/ψ daughter tracks for the vertex reconstruction. We obtain $\mathcal{S}_{J/\psi K_S^0} = 0.68 \pm 0.06(\text{stat})$, which is in agreement with the world average for $\sin 2\phi_1$ [9]. We conclude that the vertex resolution for $B^0 \rightarrow K_S^0 K_S^0$ decays is well understood. We reconstruct 1993 ± 53 $B^+ \rightarrow K_S^0 \pi^+$ [18] events and, without using the charged pion of the B decay for vertex reconstruction, apply the same fit procedure. We obtain $\mathcal{S}_{K_S^0 \pi^+} = -0.13 \pm 0.13(\text{stat})$ and $\mathcal{A}_{K_S^0 \pi^+} = 0.01 \pm 0.06(\text{stat})$, which are consistent with no CP asymmetry.

In summary, we measure time-dependent CP -violating parameters in $B^0 \rightarrow K_S^0 K_S^0$ decays, which are dominated by flavor-changing $b \rightarrow d\bar{s}s$ penguin transitions, based on a data sample of 657×10^6 $B\bar{B}$ pairs recorded with the Belle detector. We obtain $\mathcal{S}_{K_S^0 K_S^0} = -0.38_{-0.77}^{+0.69}(\text{stat}) \pm 0.09(\text{syst})$ and $\mathcal{A}_{K_S^0 K_S^0} = -0.38 \pm 0.38(\text{stat}) \pm 0.05(\text{syst})$. No significant CP asymmetry is found for these decays. These results are consistent with the SM prediction and also with the other measurement [4].

We thank the KEKB group for excellent operation of the accelerator, the KEK cryogenics group for efficient sole-

noid operations, and the KEK computer group and the NII for valuable computing and Super-SINET network support. We acknowledge support from MEXT and JSPS (Japan); ARC and DEST (Australia); NSFC (China); DST (India); MOEHRD, KOSEF, and KRF (Korea); KBN (Poland); MES and RFAAE (Russia); ARRS (Slovenia); SNSF (Switzerland); NSC and MOE (Taiwan); and DOE (USA).

-
- [1] Y. Grossman and M.P. Worah, Phys. Lett. B **395**, 241 (1997); D. London and A. Soni, Phys. Lett. B **407**, 61 (1997); T. Moroi, Phys. Lett. B **493**, 366 (2000); D. Chang, A. Masiero, and H. Murayama, Phys. Rev. D **67**, 075013 (2003); S. Baek, T. Goto, Y. Okada, and K. I. Okumura, Phys. Rev. D **64**, 095001 (2001).
 - [2] R. Fleischer, Phys. Lett. B **341**, 205 (1994).
 - [3] A.K. Giri and R. Mohanta, J. High Energy Phys. **11** (2004) 084.
 - [4] B. Aubert *et al.* (BABAR Collaboration), Phys. Rev. Lett. **97**, 171805 (2006).
 - [5] A. Abashian *et al.* (Belle Collaboration), Nucl. Instrum. Methods Phys. Res., Sect. A **479**, 117 (2002).
 - [6] S. Kurokawa and E. Kikutani, Nucl. Instrum. Methods Phys. Res., Sect. A **499**, 1 (2003) and other papers included in this volume.
 - [7] A.B. Carter and A.I. Sanda, Phys. Rev. Lett. **45**, 952 (1980); A.B. Carter and A.I. Sanda, Phys. Rev. D **23**, 1567 (1981); I.I. Bigi and A.I. Sanda, Nucl. Phys. **B193**, 85 (1981).
 - [8] Z. Natkaniec *et al.* (Belle SVD2 Group), Nucl. Instrum. Methods Phys. Res., Sect. A **560**, 1 (2006).
 - [9] W.-M. Yao *et al.*, J. Phys. G **33**, 1 (2006).
 - [10] G.C. Fox and S. Wolfram, Phys. Rev. Lett. **41**, 1581 (1978); The modified moments used in this Letter are described in S.H. Lee *et al.* (Belle Collaboration), Phys. Rev. Lett. **91**, 261801 (2003).
 - [11] H. Kakuno *et al.*, Nucl. Instrum. Methods Phys. Res., Sect. A **533**, 516 (2004).
 - [12] Events are generated with the Evtgen generator, D.J. Lange, Nucl. Instrum. Methods Phys. Res., Sect. A **462**, 152 (2001); the detector response is simulated with GEANT, R. Brun *et al.*, GEANT 3.21, CERN Report No. DD/EE/84-1, 1984.
 - [13] H. Albrecht *et al.* (ARGUS Collaboration), Phys. Lett. B **241**, 278 (1990).
 - [14] K. Sumisawa *et al.* (Belle Collaboration), Phys. Rev. Lett. **95**, 061801 (2005).
 - [15] H. Tajima *et al.*, Nucl. Instrum. Methods Phys. Res., Sect. A **533**, 370 (2004).
 - [16] O. Long, M. Baak, R. N. Cahn, and D. Kirkby, Phys. Rev. D **68**, 034010 (2003).
 - [17] S.-W. Lin *et al.* (Belle Collaboration), Phys. Rev. Lett. **98**, 181804 (2007).
 - [18] Throughout this Letter, the inclusion of the charge-conjugate decay mode is implied unless otherwise stated.